

A Preorganized Active Site in the Crystal Structure of the *Tetrahymena* Ribozyme

Barbara L. Golden,* Anne R. Gooding, Elaine R. Podell, Thomas R. Cech*

Group I introns possess a single active site that catalyzes the two sequential reactions of self-splicing. An RNA comprising the two domains of the *Tetrahymena thermophila* group I intron catalytic core retains activity, and the 5.0 angstrom crystal structure of this 247-nucleotide ribozyme is now described. Close packing of the two domains forms a shallow cleft capable of binding the short helix that contains the 5' splice site. The helix that provides the binding site for the guanosine substrate deviates significantly from A-form geometry, providing a tight binding pocket. The binding pockets for both the 5' splice site helix and guanosine are formed and oriented in the absence of these substrates. Thus, this large ribozyme is largely preorganized for catalysis, much like a globular protein enzyme.

A group I intron contains an active site that allows it to excise itself from a precursor RNA and ligate the flanking exons, generating an intact messenger RNA, transfer RNA, or ribosomal RNA (rRNA) (1). This self-splicing reaction is efficient and accurate, and it requires only sufficient magnesium ion (~2 mM) to fold the RNA and a guanosine nucleoside cofactor (1). The structure of group I introns has been extensively investigated by comparative sequence analysis of phylogenetically distinct family members (2, 3) and by site-specific mutagenesis (4). These studies identified a series of conserved elements of secondary structure (designated P1 through P9 in Fig. 1A) organized into three domains, P1-P2, P4-P6, and P3-P9 (3, 5). The catalytic core is located at the junction of the P4-P6 and P3-P9 domains. The 5' splice site is found in the P1-P2 or substrate domain. Nonconserved peripheral elements, such as the P5abc extension in the *Tetrahymena thermophila* rRNA intron, provide additional stabilization of the active structure (6).

The 5' splice site phosphate follows a uridine recognized in the context of a U·G wobble pair within the short hairpin duplex, P1. Docking of P1 into the ribozyme core involves the J4/5 and J8/7 joining regions of the intron (3, 7-9). The guanosine-binding site (within P7) binds a guanosine nucleoside and activates its 3' hydroxyl for the first transesterification reaction, which liberates the 5' exon and links the guanosine substrate to the 5' end of the intron. An obligate con-

formational change must then occur, in which the exogenous guanosine exits the active site and is replaced by a conserved guanosine (ω G) at the 3' terminus of the intron (10, 11). The 5' exon can then attack at the 3' splice site in a transesterification reaction that is chemically equivalent to the reverse of the first step of splicing. This ligates the exons and releases the intron.

Table 1. Phasing statistics. Crystals of the ribozyme core were prepared as previously described (13). The crystals belong to the space group $P4_22_1$ and have unit-cell dimensions $a = b = 179.0$ Å, $c = 199.3$ Å. For data collection, crystals were cryostabilized for 24 to 48 hours in 15% ethanol, 25% 2,5-methylpentane-diol (MPD), 50 mM potassium cacodylate, 50 mM KCl, 50 mM $MgCl_2$, and 0.5 mM spermine. Lanthanide derivatives were prepared by cocrystallization with 0.2 mM $Sm(Ac)_3$ or $EuCl_3$ and cryostabilization with 0.2 to 0.4 mM lanthanide. Osmium hexammine derivatives were made by cocrystallization with 0.5 mM cobalt hexammine followed by exchange into 0.5 to 1.0 mM osmium hexammine in cryostabilization buffer (15). Crystals were flash frozen in propane and mounted in an Oxford cryostream (100 K) for data collection. Data were collected at the National Synchrotron Light Source, Brookhaven National Laboratory, beamline X25 using the Brandeis B4 charge-coupled-device detector, and were indexed and scaled using the HKL package (42). The lanthanide positions were determined by manual inspection of Patterson maps. Osmium hexammine sites were located in difference Fourier maps. Phase calculations and solvent flattening were performed using PHASES (43). Both MIRAS and MAD data [treated as a special form of MIR (44)] were used to calculate electron density maps. Most of the phasing power is contributed from the anomalous data. Model building was accomplished with the program O (45). The CNS package was used for rigid-body refinement and energy minimization of the model (46). Crystallographic refinement is not feasible at this resolution. Iso./disp., isomorphous or dispersive; Anom., anomalous.

Dataset	λ (Å)	Resolution (Å)	Completeness (%)	R_{sym}^* (%)	R_{merge} (%)		Phasing power†	
					Iso./disp.	Anom.	Iso./disp.	Anom.
Native	1.0000	5.00	99.2	5.2	—	—	—	—
EuCl ₃	1.7748	5.50	94.9	5.6	15.2	6.3	1.34	2.20
SmAc	1.8438	5.70	99.1	6.1	10.4	7.2	1.34	2.03
OsHex	1.1403	5.00	98.4	5.5	11.4	5.2	1.14	2.23
SmAc (λ 1)	1.8433	5.50	93.2	7.3	—	—	—	—
SmAc (λ 2)	1.8439	5.50	94.4	6.5	6.6	6.5	0.13	1.45
SmAc (λ 3)	1.8287	5.50	93.2	6.8	6.4	4.4	0.63	1.34
OsHex (λ 1)	1.1407	5.00	99.4	4.6	—	—	—	—
OsHex (λ 2)	1.1400	5.00	99.3	5.0	4.1	6.8	0.16	2.50
OsHex (λ 3)	1.1190	5.00	99.3	4.6	4.6	4.1	1.08	2.70

Overall figure of merit: 0.603. $*R_{sym} = \sum |I - \langle I \rangle| / \sum \langle I \rangle$. †Phasing power is F_{iso}/E for the isomorphous or dispersive case and $2F_{an}/E$ for the anomalous case.

Howard Hughes Medical Institute, Department of Chemistry and Biochemistry, University of Colorado, Boulder, CO 80309-0215, USA.

*To whom correspondence should be addressed. E-mail: bgolden@petunia.colorado.edu (B.L.G.); Thomas.Cech@colorado.edu (T.R.C.).

There has been an effort in recent years to study structure-function relationships, in the group I introns using x-ray crystallography. The structure of one of the domains of the *Tetrahymena* rRNA intron, P4-P6, was solved 2 years ago and revealed interactions that allow large RNAs to form closely packed structures (12). To build upon this result, we designed an RNA that encompasses both the P4-P6 and P3-P9 domains of this intron, thereby completing the group I catalytic core (13). This molecule also includes ω G, which serves as an internal guanosine nucleophile. The resulting RNA is catalytic; it binds the P1-P2 domain purely through tertiary interactions and, using ω G, cleaves the P1 duplex at positions that are consistent with the activity of the full-length intron. By systematic mutation of peripheral regions of the molecule, we were able to introduce a crystal contact and thereby obtain crystals that diffract isotropically to ~5 Å.

Global architecture. The crystal structure of this 247-nucleotide group I ribozyme was solved at 5.0 Å resolution using three heavy-atom derivatives (Table 1 and Fig. 1B) (14). At this resolution, there is clear density for the backbone and some indication of where the monomeric units are positioned (Fig. 2). Stacked bases are often seen as continuous tubes of density. Atomic-level interactions such as hydrogen bonding cannot

RESEARCH ARTICLE

be defined at this resolution. However, spatial proximities can be determined and used to propose specific interactions that can be tested in the future.

Within the ribozyme crystal structure, the P4-P6 domain appears largely unchanged from the previously determined 2.8 Å structure of the isolated domain (12). This is apparent from the preservation of heavy-atom binding sites (Table 2) (15) and from the experimental electron density map (16). The P4-P6 domain is hairpin shaped, consisting of two coaxially stacked helical regions separated by a sharp bend (Fig. 3A). The maintenance of the three-dimensional (3D) structure of this RNA domain in two different molecular contexts (as a free domain and as a portion of an active ribozyme) and in completely different crystal packing arrangements is encouraging for the field of large RNA crystallography.

The P3-P9 domain, which had not been crystallized previously, wraps around the P4-P6 domain. It makes an extensive and intimate interface with P4-P6, completing the active site of the intron (Fig. 3). Within the folded structure, the surface area buried by this domain-domain interaction was calculated to be $\sim 1475 \text{ \AA}^2$ (17). P3-P9 is composed of five helices. In the structure, four of these (P8, P3, P7, and P9.0) are coaxially stacked to form a bent pseudocontinuous helix. The bend, localized between the P3 and P7 helices and within P7 itself, is $\sim 50^\circ$. The P9 helix is not coaxial with the others, making a $\sim 90^\circ$ bend to interact with the minor groove face of P5 within the P4-P6 domain. Of the helical elements within the P3-P9 domain, only P8 lacks a significant interface with the P4-P6 domain.

The ribozyme is much wider than a single A-form helix in every dimension. The height of the ribozyme is the same as that of the isolated P4-P6, $\sim 110 \text{ \AA}$ tall (12). The ribozyme is about 65 Å wide at the junction of the two domains. The P3-P9 domain is $\sim 95 \text{ \AA}$ tall and one helix wide throughout its most of its length, although the bends give it a larger width overall. As a comparison, the restriction endonuclease Eco RI, which also recognizes a nucleic acid duplex, is a dimer with dimensions of only ~ 40 to 60 Å in each direction (18). The size difference between the enzyme

and the ribozyme suggests that it may be possible to build an active site more efficiently using amino acids than nucleotides.

The crystals contain two molecules of the ribozyme per asymmetric unit. The conformation of these molecules is nearly identical

except at the very 3' terminus. The close similarity of the core of these two molecules in spite of different crystallographic environments suggests that the active-site structure is stable and not very susceptible to deformation. One molecule (molecule A) has ωG

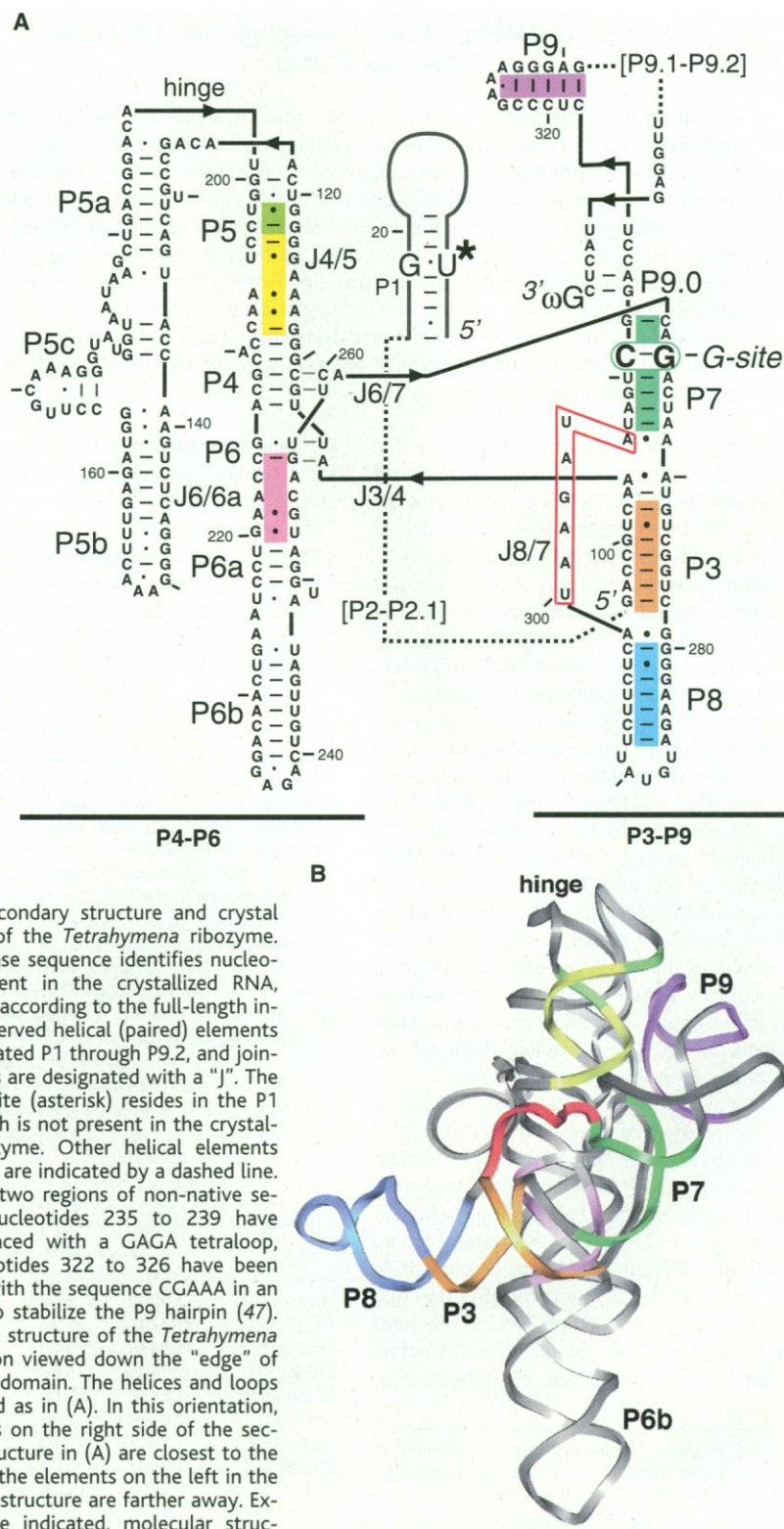


Fig. 1. Secondary structure and crystal structure of the *Tetrahymena* ribozyme. (A) The base sequence identifies nucleotides present in the crystallized RNA, numbered according to the full-length intron. Conserved helical (paired) elements are designated P1 through P9.2, and joining regions are designated with a "J". The 5' splice site (asterisk) resides in the P1 helix, which is not present in the crystallized ribozyme. Other helical elements not shown are indicated by a dashed line. There are two regions of non-native sequence: nucleotides 235 to 239 have been replaced with a GAGA tetraloop, and nucleotides 322 to 326 have been replaced with the sequence CGAAA in an attempt to stabilize the P9 hairpin (47). (B) Crystal structure of the *Tetrahymena* rRNA intron viewed down the "edge" of the P4-P6 domain. The helices and loops are colored as in (A). In this orientation, the helices on the right side of the secondary structure in (A) are closest to the front, and the elements on the left in the secondary structure are farther away. Except where indicated, molecular structures were generated with Insight II (Biosym Technologies, San Diego, California).

Table 2. Interatomic distances between heavy atoms (in angstroms).

RNA	Eu-Os1	Eu-Os2	Os1-Os2
P4-P6 (15)	25.8	32.4	30.7
Molecule A*	25.7	33.2	30.5
Molecule B*	24.1	32.3	30.6

*The two 247-nucleotide ribozymes in the asymmetric unit.

docked in or near the guanosine-binding site in P7, as expected. In the second molecule (molecule B), the last nine nucleotides are in a non-native conformation; the penultimate

eight residues form a double helix with a symmetry-related molecule via perfect Watson-Crick complementarity. This leaves the guanosine-binding site of the molecule unoccu-

pled and places ω G in the vicinity of the P1-binding site of the ribozyme.

Organization of the interdomain junction. Inspection of the secondary structures of group I introns shows that the junction of the two domains involves the close approach of the P4, P6, P3, and P7 helices (Fig. 1A). Assembly of these helices into a catalytic conformation is mediated in part by base triples involving J3/4 and J6/7 (19, 20). In the ribozyme structure, the electron density for the RNA backbone supports the presence of the expected triple helical array. This is in contrast to the crystal structure of the isolated P4-P6 domain, where this scaffold of base triples is not formed as predicted (12), due in part to a crystal contact. Independent evidence for this change in structure is the loss of an osmium hexamine-binding site involving nucleotides A256 and G257 in going from the isolated domain (15) to the ribozyme. This suggests that these ligands to this heavy atom have shifted position.

The three residues of the J3/4 segment link the two domains of the ribozyme core. The first residue, A104, stacks directly upon the P3 helix and is in a position to form a potential quartet with A270, C217, and A256, thereby bridging the P3-P9 and P4-P6 domains. The final two, A105 and U106, appear to be involved in the minor groove triples predicted by comparative sequence analysis of phylogenetically distinct RNAs (Fig. 1A) (19).

The P3 helix stacks directly beneath the J3/4 linker and is oriented by minor groove interdigitation with J6/6a in the P4-P6 domain (Fig. 4). J6/6a is double-helical, presumably held together by non-Watson-Crick base pairs. It has a widened minor groove that appears to facilitate its interaction with P3. A U·U base pair in P3 provides a constriction in this helix that may accommodate the close approach of backbones in this region. The structure of J6/6a within the ribozyme differs from its structure in the isolated P4-P6 domain where the J6/6a internal loop is involved in a crystal contact, forming a base platform that allows the non-native tertiary contact (21).

A series of interactions contributes to orientation of the P7 helix. The minor-groove base triples involving J3/4 help to bridge the interaction between P7 and P4. The 5' strand of P7 and residues 104 through 107 within J3/4 and P4 are characterized by a very close approach of phosphate groups of the RNA backbone. The conformation in this region is reminiscent of the structure seen in loop E of 5S rRNA (22), where well-ordered magnesium ions bridge the close approach of the backbone. Although we cannot place magnesium ions with confidence at this resolution, there is density in $|F_o - F_c|$ maps for potential magnesium ligands at several of these

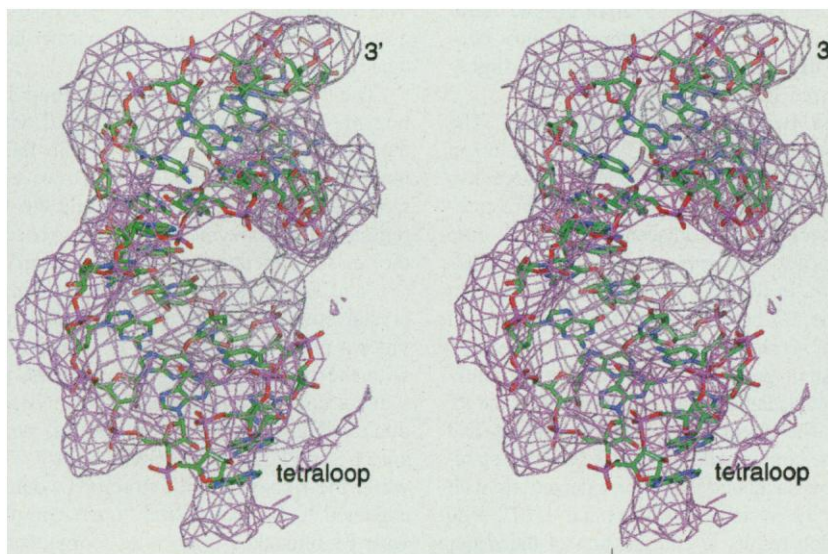


Fig. 2. The solvent-flattened experimental electron density map (pink net) in the vicinity of helix P5b, calculated at 5 Å resolution and contoured at 1σ . Atoms are colored as follows: green, carbon; blue, nitrogen; red, oxygen; violet, phosphate.

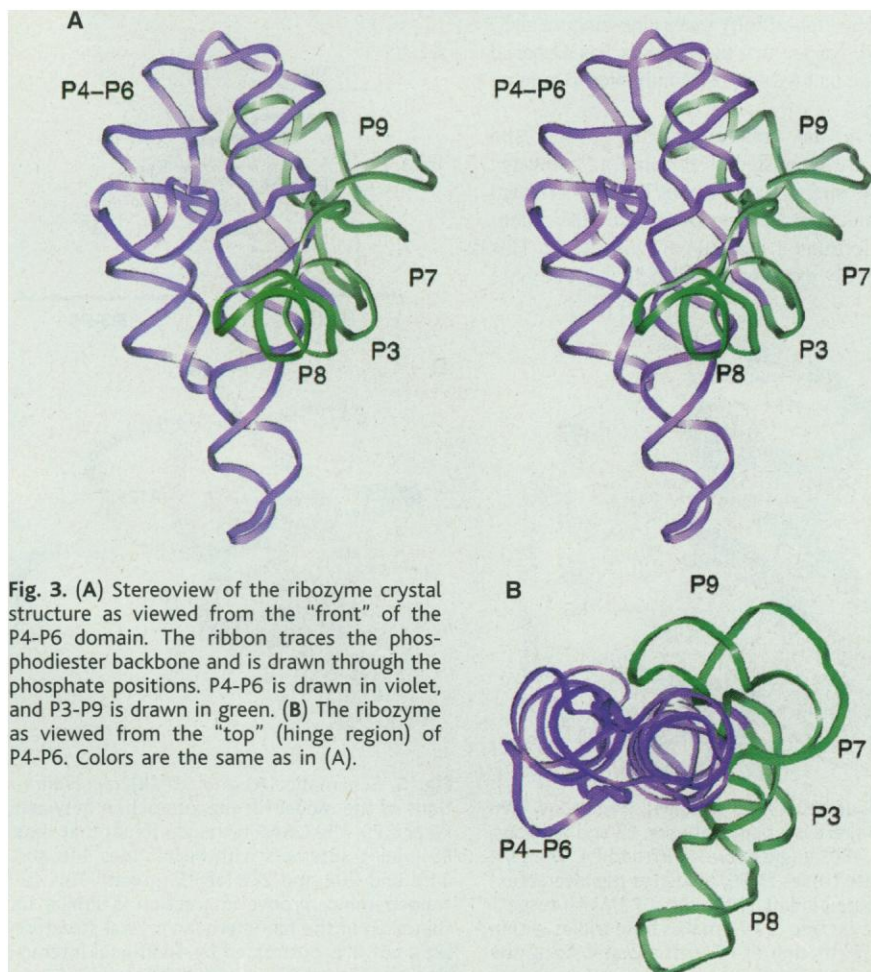


Fig. 3. (A) Stereoview of the ribozyme crystal structure as viewed from the "front" of the P4-P6 domain. The ribbon traces the phosphodiester backbone and is drawn through the phosphate positions. P4-P6 is drawn in violet, and P3-P9 is drawn in green. (B) The ribozyme as viewed from the "top" (hinge region) of P4-P6. Colors are the same as in (A).

positions. Additionally, at many of these nucleotides, substitution of phosphorothioates, which disrupts Mg^{2+} binding, is inhibitory to catalysis (23).

Base triples involving the J6/7 region of the intron also help to orient the P7 helix. The J6/7 region is a three-nucleotide spacer that must span the length of P7 (Fig. 1), and thus limits the orientation of the guanosine-binding site with respect to P4-P6. The first two nucleotides in J6/7 are involved in major groove triples to P4 (19). The last nucleotide, A261, bridges the gap to the top of P7.

An interdomain strut. Tetraloops are a recurring motif in RNA secondary structure and can often mediate tertiary interactions (3, 12, 24, 25). In the current structure, the L9 tetraloop is located in proximity to P5. L9 was modeled as a standard GAAA tetraloop (25, 26). The resulting orientation has the tetraloop docked into the minor groove of P5 at base pairs G118 through C203 and G119 through U202, in accordance with a previous prediction (3). The importance of this interaction is supported by site-specific disruption of this interdomain tertiary contact (27), which significantly destabilizes the intron. Protection of P5 by P9 occurs as an early step in the folding of the P3-P9 domain (28), suggesting this interaction may be important for the kinetic folding pathway as well as the stability of the folded structure.

In the ribozyme crystal structure, there is potential for additional interactions between L9 and the hinge region of P4-P6 (Fig. 5). In particular, A125 is in a position to stack upon the tetraloop. It has been noted that replacement of the P4-P6 hinge region with oligouridine is somewhat destabilizing and, while sufficient to fold the P4-P6 domain at mod-

erate magnesium ion concentrations, does not restore full catalytic activity (29). This supports the notion that the hinge region, as well as the base pairs in P5, serve to form a more complex "receptor" for L9 than previously predicted. Buttressing of minor groove-tetraloop interactions by additional tertiary contacts may be a common theme in highly structured RNAs.

The two substrate-binding sites. The guanosine-binding site (G site) of the intron is located within the P7 helix, where hydrogen-bonding promotes nucleophile recognition (10). The adjacent A265-U310 base pair has also been implicated in guanosine binding (30). In the crystal structure, it is apparent that the P7 helix deviates significantly from A-form geometry (Fig. 6A). This is likely due, at least in part, to A263, which is currently modeled as unpaired and stacked within the P7 helix. The orientation of this nucleotide, and thus the conformation of P7, is probably stabilized by backbone-backbone interactions with P4 in the vicinity of U106 and U107. The distortion results in compression of the major groove and provides a snug binding site for the guanosine substrate (31). This finding may explain a previous conundrum: if guanosine binding only required two specific base pairs in a helix, many double-stranded regions of RNA would be high-affinity guanosine-binding sites. Instead, we see that the P7 helix has a special structure that we propose contributes to binding affinity.

From the crystal structure, A306 and A261 are identified as forming a "gateway" to the G site. A306 of the J8/7 single-stranded region is stacked beneath residue 307, potentially forming a sheared pair with A269. This effectively extends the P7 helix by one base

pair and places A306 well within the G site. This also explains the strong conservation of A306 and residues at the bottom of P7 (including U307 and A308) which are adjacent to the guanosine substrate in the 3D structure. The resulting geometry also places A261 quite close in space to the other partner in the "gateway."

The second substrate of the group I ribozyme is the 5' splice site, located within the P1 duplex. P1 is not present in the ribozyme that was crystallized. However, a model for the interaction of P1 and the J4/5 region of the ribozyme has been proposed on the basis of functional group substitution data (9), and superposition of this model on the crystal structure of the ribozyme now provides a preliminary view of P1's interaction with the ribozyme core. The ribozyme provides a concave binding site for an A-form duplex (Fig. 6B). The "sides" of this pocket are J4/5 and P3, and the "floor" is J8/7. Thus, while the ribozyme core structure would be expected to be that of the "open complex" with P1 undocked (32), little reorganization of the core is required to accommodate binding of P1.

The connecting strand J8/7 is also involved in binding P1 (8), and its conformation in the crystal is consistent with it con-

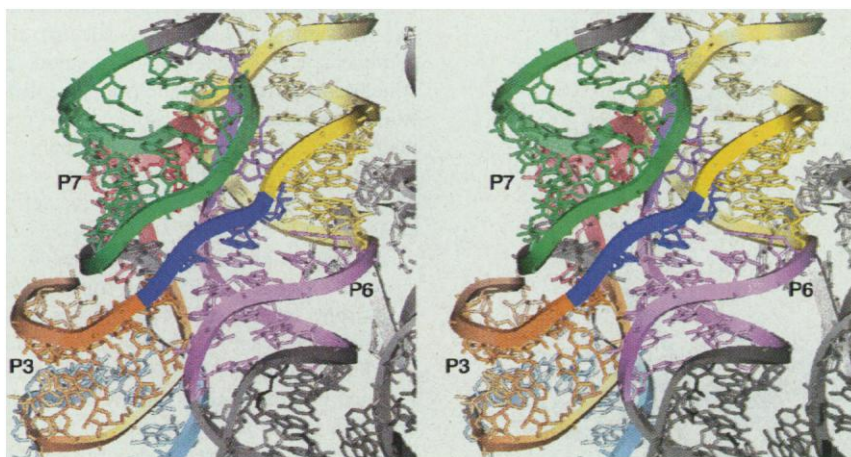


Fig. 4. The ribozyme core is formed by the junction of four helices, P3 (orange), P4 (yellow), P6 (pink), and P7 (green). P4 and P6 are coaxially stacked, but there is a bend between P3 and P7. Thus, while P3 and P6 are nearly perpendicular, there is only a $\sim 30^\circ$ angle between P7 and P4. The J3/4 segment (dark blue), which is involved in minor-groove base triples to P6, mediates the interaction between P7 and P6, thereby helping to orient the guanosine binding site (within P7) with respect to the P4-P6 domain. The second linker, J6/7 (violet, on the far side of P7), makes base triples within the major groove of P4 and also helps to define the conformation of P7, perhaps stabilizing the bend within this helix.

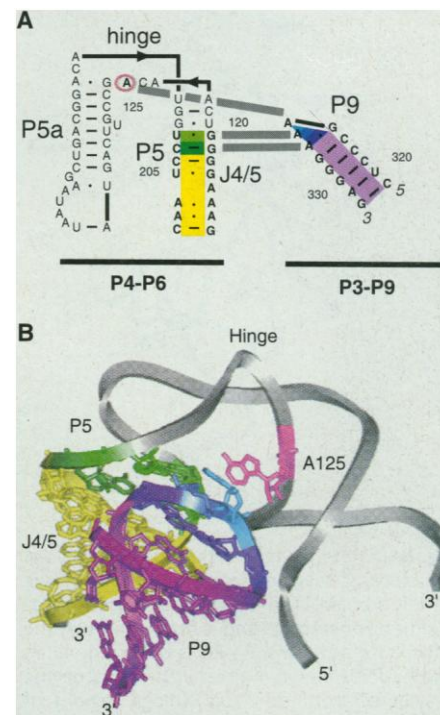


Fig. 5. Schematic (A) and 3D (B) representations of the model for the interaction between P5 and P9. The GAAA tetraloop (blue) that caps P9 (violet) interacts with nucleotides 118 and 119, and 202 and 203 of P5 (green). This tetraloop-minor groove interaction is similar to that seen in the hammerhead crystal structure (25), but it is buttressed by additional interactions such as stacking with A125 (pink).

tributing to such a binding site. The first three nucleotides of J8/7 (nucleotides 300 through 302) are stacked with nearly A-form geometry. This conformation is stabilized by interactions between two adenosine bases in J8/7 (nucleotides 301 and 302) and the backbone of P3 (near A269). This base-backbone interaction may be mediated by a magnesium ion, which is supported by solution-probing data (33). Following residue 302, a sharp bend points the bases of residues 303 and 304 out, toward P1. The next J8/7 base, U305, is then in position to make the major-groove triple with base pair 5 of P4, as proposed from site-specific mutational analysis (34). In this model for the P1-ribozyme interaction, the phosphate that defines the 5' splice site is well-placed with respect to the binding site for the guanosine nucleophile (Fig. 6A).

Group I introns are metalloenzymes and require divalent metal ions, Mg^{2+} or Mn^{2+} , for catalysis (35). Even at 5 Å resolution, it is tempting to speculate which functional groups within the active site could bind to the metals that participate in catalysis. There are four phosphate positions—A306, A261, A207, and C208—that span the “gateway” to the guanosine-binding site. These phosphate groups have previously been identified as sites of phosphorothioate interference (23). When P1 is docked as described above, these four groups surround the phosphate at the 5' splice site. These are excellent candidates for ligands to catalytic metals, and further biochemical analysis will test this proposal.

Comparisons with previous data. All of the helices that were predicted to form by phylogeny and mutational analyses (3, 4) could be modeled into the experimental electron density map. Furthermore, many of the positions along the backbone that are sensitive to phosphorothioate substitution (23) are at the domain interface. Electron microscopy of the full-length *Tetrahymena* intron revealed a globular molecule with a diameter of ~116 Å (36). Considering that the P1-P2 domain and helices P9.1 and P9.2 are deleted, the dimensions of the ribozyme in the crystal structure are consistent with the electron micrographs. Introns in which P6b and P8 were extended by ~80 base pairs were also visualized by electron microscopy (37). This allowed the angle between these two helical elements to be estimated as ~90°, in agreement with the angle measured in the crystal structure.

It has been proposed that modeling of 3D structure from sequence information might be more successful for RNA than for protein because of the hierarchical nature of RNA folding: sequence determines a very stable secondary structure, which is then maintained when tertiary structure forms. Michel and Westhof constructed a model of the *Tetrahymena* ribozyme core based mainly on comparative sequence analysis and stereochemical constraints, with biochemical testing of certain proposed interactions (3, 38). The overall architecture of the Michel-Westhof model agrees extremely well with the crystal structure; local interactions sometimes differ,

especially in the regions where the sequence is highly conserved or where the interactions are not Watson-Crick pairing. The overall agreement should be considered a real triumph for RNA modeling: it is possible to predict a 3D fold of an RNA in the absence of any solved structure of a related molecule.

A continuing concern in RNA crystallography is crystallization of a conformation that deviates significantly from the catalytically relevant structure (39). This concern arises both from solution studies that reveal RNA enzymes to be much more dynamic than their protein counterparts (40) and from crystallographic investigations that reveal native secondary, but not tertiary structures (41). It is therefore encouraging to see that the crystal structure of the *Tetrahymena* ribozyme core is consistent with a large body of biochemical data. The relevant structure is retained in the absence of the P1-P2 domain, and, in the case of molecule B, in the absence of bound guanosine. Thus, in contrast to the small ribozymes, such as the hammerhead RNA, group I introns appear to be largely preorganized to bind their substrates.

References and Notes

1. K. Kruger *et al.*, *Cell* **31**, 147 (1982); reviewed by R. Saldanha, G. Mohr, M. Belfort, A. M. Lambowitz, *FASEB J.* **7**, 15 (1993) and by T. R. Cech, in *The RNA World*, R. F. Gesteland and J. F. Atkins, Eds. (Cold Spring Harbor Laboratory Press, Cold Spring Harbor, NY, 1993), pp. 239–269.
2. F. Michel, A. Jacquier, B. Dujon, *Biochimie* **64**, 867 (1982); R. W. Davies, R. B. Waring, J. A. Ray, T. A. Brown, C. Scazzocchio, *Nature* **300**, 719 (1982); T. R. Cech, *Gene* **73**, 259 (1988).
3. F. Michel and E. Westhof, *J. Mol. Biol.* **216**, 585 (1990).
4. R. B. Waring, J. A. Ray, S. W. Edwards, C. Scazzocchio, R. W. Davies, *Cell* **40**, 371 (1985); J. M. Burke *et al.*, *ibid.* **45**, 167 (1986); S. Couture *et al.*, *J. Mol. Biol.* **215**, 345 (1990); reviewed by J. M. Burke, *Gene* **73**, 273 (1988).
5. F. L. Murphy and T. R. Cech, *Biochemistry* **32**, 5291 (1993); T. R. Cech, S. H. Damberger, R. R. Gutell, *Nature Struct. Biol.* **1**, 273 (1994).
6. G. F. Joyce, G. van der Horst, T. Inoue, *Nucleic Acids Res.* **17**, 7879 (1989); G. van der Horst, A. Christian, T. Inoue, *Proc. Natl. Acad. Sci. U.S.A.* **88**, 184 (1991); B. Laggenbauer, F. L. Murphy, T. R. Cech, *EMBO J.* **13**, 2669 (1994).
7. J. F. Wang, W. D. Downs, T. R. Cech, *Science* **260**, 504 (1993).
8. A. M. Pyle, F. L. Murphy, T. R. Cech, *Nature* **358**, 123 (1992).
9. S. A. Strobel, L. Ortoleva-Donnelly, S. P. Ryder, J. H. Cate, E. Moncoeur, *Nature Struct. Biol.* **5**, 60 (1998).
10. F. Michel, M. Hanna, R. Green, D. Bartel, J. W. Szostak, *Nature* **342**, 391 (1989).
11. M. D. Been and A. Perrotta, *Science* **252**, 434 (1991).
12. J. H. Cate *et al.*, *ibid.* **273**, 1678 (1996).
13. B. L. Golden, E. R. Podell, A. R. Gooding, T. R. Cech, *J. Mol. Biol.* **270**, 711 (1997).
14. Europium, samarium, and osmium hexammine derivatives were used to calculate an electron density map domain (Table 1). These compounds are known to bind to P4-P6 (12, 15). In the new structure, four of the five binding sites for these heavy atoms are preserved. Using the distances between heavy-atom positions (Table 2), the locations of the two P4-P6 domains within the asymmetric unit could be deduced. These locations were then confirmed by examination of the electron density map. Using the location of the P4-P6 domain as a foothold, the P3-P9

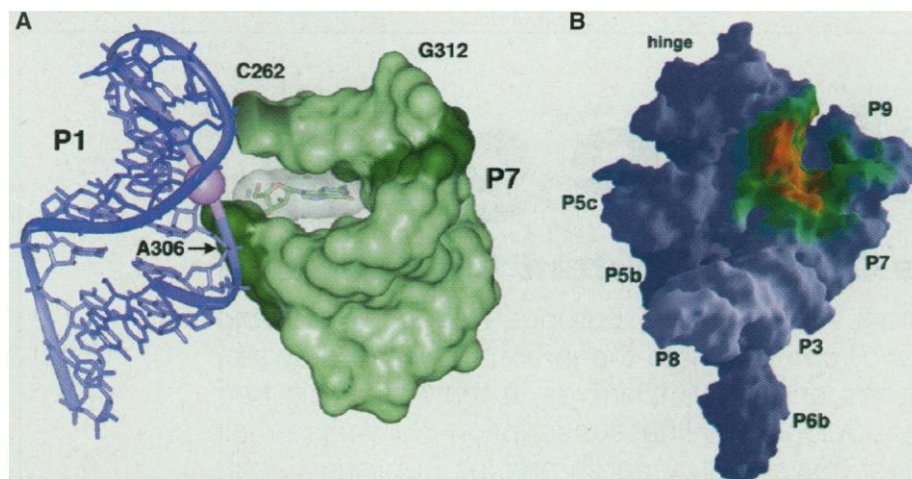


Fig. 6. (A) The model for P1's interaction with the ribozyme juxtaposes the guanosine-binding site and the 5' splice site. The nuclear magnetic resonance structure of P1 (48) was positioned relative to J4/5 using the model of Strobel *et al.* (9). The resulting model places the 5' splice site in close proximity to the guanosine substrate-binding site within P7. The P7 helix (green) is represented as a surface with the G264-C311 base pair highlighted in darker green. One of the “gateway” nucleotides, A306, is also rendered in dark green. For reference, a guanosine molecule has been placed within hydrogen-bonding distance of G264 (10), although its precise orientation, and therefore the distance between the guanosine 3'-hydroxyl and 5' splice site, is not well determined at this resolution. The P1 duplex is shown in blue, and the phosphate at the 5' splice site is shown as a pink CPK (Corey-Pauling-Koltun) atom. (B) A shallow cleft on the ribozyme forms the P1 binding site. The molecular surface of the ribozyme was created using GRASP (17), and the contacts to P1 [modeled as in (A)] are highlighted. Red represents direct contacts, and green represents the surface within 3 Å of P1.

- domain could then be built into the electron density map with confidence, assuming near A-form geometry and stacking interactions wherever consistent with the electron density. In this manner, it was possible to derive a model that included all the nucleotides in both molecules of the asymmetric unit (Fig. 1B).
15. J. H. Cate and J. A. Doudna, *Structure* **4**, 1221 (1996).
 16. Two significant differences from the previous crystal structure are evident. There is a slight bend in the P6b helix that permits a crystal contact within the dimer that makes up the asymmetric unit of the ribozyme crystals. Additionally, there is a rearrangement of residues at the interdomain junction.
 17. A. Nichols, K. Sharp, B. Honig, *Proteins Struct. Funct. Genet.* **11**, 281 (1991).
 18. Y. C. Kim, J. C. Grable, R. Love, P. J. Greene, J. M. Rosenberg, *Science* **249**, 1307 (1990).
 19. F. Michel, A. D. Ellington, S. Couture, J. W. Szostak, *Nature* **347**, 578 (1990).
 20. W. D. Downs and T. R. Cech, *RNA* **2**, 718 (1996); P. P. Zarrinkar and J. R. Williamson, *Nature Struct. Biol.* **3**, 432 (1996).
 21. J. H. Cate et al., *Science* **273**, 1696 (1996).
 22. C. C. Corell, B. Freeborn, P. B. Moore, T. A. Steitz, *Cell* **91**, 705 (1997).
 23. E. L. Christian and M. Yarus, *J. Mol. Biol.* **228**, 743 (1992); *Biochemistry* **32**, 4475 (1993); L. Ortoleva-Donnelly, A. A. Szewczak, R. R. Gutell, S. A. Strobel, *RNA* **4**, 498 (1998).
 24. F. L. Murphy and T. R. Cech, *J. Mol. Biol.* **236**, 49 (1994); M. Costa and F. Michel, *EMBO J.* **14**, 1276 (1995).
 25. H. W. Pley, K. M. Flaherty, D. B. McKay, *Nature* **372**, 111 (1994).
 26. H. A. Heus and A. Pardi, *Science* **253**, 191 (1991); F. M. Jucker, H. A. Heus, P. F. Yip, E. H. Moors, A. Pardi, *J. Mol. Biol.* **264**, 968 (1996).
 27. M. G. Caprara and R. B. Waring, *Gene* **143**, 29 (1994).
 28. B. Sclavi, M. Sullivan, M. R. Chance, M. Brenowitz, S. A. Woodson, *Science* **279**, 1940 (1998).
 29. A. A. Szewczak and T. R. Cech, *RNA* **3**, 838 (1997).
 30. M. Yarus, M. Illangsekare, E. Christian, *J. Mol. Biol.* **222**, 995 (1991).
 31. It is evident that ω G is docked in the guanosine-binding site in molecule A, but the orientation of this nucleotide is not well determined by the x-ray data. However, we believe that compression of the P7 helix prevents guanosine from binding in a geometry coplanar with the G264-C311 base pair. A more axial position for guanosine (30) is tolerated in the model and would allow a more extensive set of hydrogen bonds to the nucleoside.
 32. P. C. Bevilacqua, R. Kierzek, K. A. Johnson, D. H. Turner, *Science* **258**, 1355 (1992); D. Herschlag, *Biochemistry* **31**, 1386 (1992).
 33. T. McConnell, thesis, University of Colorado (1995); C. Berens, B. Streicher, R. Schroeder, W. Hillen, *Chem. Biol.* **5**, 163 (1998).
 34. M. A. Tanner and T. R. Cech, *Science* **275**, 847 (1997); M. A. Tanner, E. M. Anderson, R. R. Gutell, T. R. Cech, *RNA* **3**, 1037 (1997).
 35. J. A. Piccirilli, J. S. Vyle, M. H. Caruthers, T. R. Cech, *Nature* **361**, 85 (1993); T. A. Steitz and J. A. Steitz, *Proc. Natl. Acad. Sci. U.S.A.* **90**, 6498 (1993); A. S. Sjögren, E. Pettersson, B.-M. Sjöberg, R. Stromberg, *Nucleic Acids Res.* **25**, 648 (1997); L. B. Weinstein, B. C. Jones, R. Costick, T. R. Cech, *Nature* **388**, 805 (1997).
 36. Y. H. Wang, F. L. Murphy, T. R. Cech, J. D. Griffith, *J. Mol. Biol.* **236**, 64 (1994).
 37. T. M. Nakamura, Y.-H. Wang, A. J. Zaig, J. D. Griffith, T. R. Cech, *EMBO J.* **14**, 4849 (1995).
 38. V. Lehnert, L. Jaeger, F. Michel, E. Westhof, *Chem. Biol.* **3**, 993 (1996).
 39. D. B. McKay, *RNA* **2**, 395 (1996).
 40. S. B. Cohen and T. R. Cech, *J. Am. Chem. Soc.* **119**, 6259 (1997).
 41. S. R. Holbrook, C. Cheong, I. Tinoco Jr., S. H. Kim, *Nature* **353**, 579 (1991); S. E. Lietzke, C. L. Barnes, J. A. Berglund, C. E. Kundrot, *Structure* **4**, 917 (1996).
 42. Z. Otwinowski, in *Proceedings of CCP4 Study Weekend: Data Collection and Processing*, L. Sawyer, N. Isaacs, S. Bailey, Eds. (SERC Daresbury Laboratory, Warrington, UK, 1993), pp. 80–86; D. Gewirth, *The HKL Manual—A Description of Programs Denzo, Xdisplay and Scalepack* (Yale University, New Haven, CT, ed. 4, 1994).
 43. W. Furey and S. Swaminathan, *Methods Enzymol.* **277**, 590 (1997); B. C. Wang, *ibid.* **115**, 90 (1985).
 44. V. Ramakrishnan and V. Biou, *ibid.* **276**, 538 (1997).
 45. T. A. Jones, J. Y. Zou, S. W. Cowan, M. Kjeldgaard, *Acta Crystallogr. A* **47**, 110 (1991).
 46. A. T. Brünger et al., *Acta Crystallogr. D*, in press.
 47. Isomorphous crystals are also obtained with the wild-type sequence in P9.
 48. F. H. Allain and G. Varani, *J. Mol. Biol.* **250**, 333 (1995).
 49. We are indebted to C. Ogata for synchrotron data collection and excellent advice. Thanks to A. Zaig, L. Berman, Z. Yin, J. Skinner, and R. Sweet for help with data collection at the X25 beamline, Brookhaven National Laboratory; M. Horvath, S. Strobel, and members of the Cech, Schultz, and Kundrot labs and the University of Colorado Structural Biology Group for advice and discussion; and the laboratory of H. Taube for the generous gift of osmium hexamine triflate. Supported by an American Cancer Society postdoctoral fellowship to B.L.G. and the Howard Hughes Medical Institute.

21 July 1998; accepted 20 August 1998

Mind the gap.

NEW! Science Online's Content Alert Service

With *Science's* Content Alert Service, European subscribers (and those around the world) can eliminate the information gap between when *Science* publishes and when it arrives in the post. This free enhancement to your *Science* Online subscription delivers e-mail summaries of the latest news and research articles published each Friday in *Science*—**instantly**. To sign up for the Content Alert service, go to *Science* Online and eliminate the gap.

Science
www.sciencemag.org

For more information about Content Alerts go to www.sciencemag.org. Click on Subscription button, then click on Content Alert button.